Nonstationary coherent optical effects caused by pulse propagation through acetylene-filled hollow-core photonic-crystal fibers

M. Ocegueda, E. Hernandez, and S. Stepanov
CICESE, Ensenada, Baja California 22860, Mexico

P. Agruzov and A. Shamray
A. F. Ioffe Physical Technical Institute, St. Petersburg 194021, Russia

(Received 28 January 2014; published 5 June 2014)

Experimental observations of nonstationary coherent optical phenomena, i.e., optical nutation, free induction, and photon echo, in the acetylene ($^{12}C_2H_2$) filled hollow-core photonic-crystal fiber (PCF) are reported. The presented results were obtained for the acetylene vibration-rotational transition $P9$ at wavelength 1530.37 nm at room temperature under a gas pressure of <0.5 Torr. An all-fiber pumped-through cell based on the commercial 2.6-m-long PCF with a 10-μm hollow-core diameter was used. The characteristic relaxation time T_2 during which the optical coherent effects were typically observed in our experiments was estimated to be ≈8 ns. This time is governed by the limited time of the acetylene molecules' presence inside the effective PCF modal area and by intermolecule collisions. An accelerated attenuation of the optical nutation oscillations is explained by a random orientation of acetylene molecules.

DOI: 10.1103/PhysRevA.89.063403 PACS number(s): 42.50.Md, 42.50.Gy, 42.70.Qs

I. INTRODUCTION

Acetylene (C_2H_2) filled hollow-core photonic-crystal fibers (PCFs) [1,2] attract considerable attention as a promising object for experimental observation and practical applications of different resonant optical nonlinear effects. Among these phenomena, which are observed at room temperature and with subwatt cw light power level, are saturation of optical absorption [2,3], electromagnetically induced transparency [2,4], and slow or fast light propagation [5,6]. An increased interest also stems from the overlap of the wavelength range of the comb of narrow vibration-rotational acetylene absorption lines (1512–1542 nm) [7,8] with the optical fiber communication spectral region. It has recently been demonstrated in [9,10] that all-fiber acetylene-filled PCF cells can be used for frequency stabilization of erbium fiber lasers.

The nonlinear effects mentioned above basically belong to the noncoherent light-molecule interactions and are typically observed during the illumination times, which are significantly longer than the characteristic time of the molecule memory about the incident excitation light wave phase, i.e., the transverse relaxation time T_2 [11]. The electromagnetically induced transparency (a quantum superposition of two lower-energy states in a three-level system) is the only coherent optical effect that was demonstrated in PCFs. However, this is a stationary process which is observed at excitation by two cw laser fields. On the contrary, the nonstationary coherent optically nonlinear effects, such as optical nutation, free induction, photon echo, or self-induced transparency [11], are typically observed at pulse excitation during the time intervals shorter than T_2 or comparable with it.

It is usually assumed (see, e.g., [2,3,5]) that the characteristic relaxation time T_2 in acetylene-filled PCF cells is governed by collisions between acetylene molecules (at high gas pressures) or by collisions of freely flying molecules with internal walls of the PCF hollow core. For room temperature, when the mean thermal acetylene molecule velocity is about 500 km/s [2,3], low gas pressure, and for typical hollow-core diameter of 10 μm the minimal possible relaxation time T_2 can roughly be estimated as ∼20 ns. This value was reported for direct measurements of the saturated spectral hole widths (40–50 MHz) published in [3,5]. This evaluation predicts that the nonstationary optical coherent effects can be expected for observation time <20 ns and at rather high laser peak powers (≥1 W) which have not been used in the experimental studies of acetylene-filled PCFs earlier. Below in this paper we report experimental observation of the nonstationary optical coherent effects, such as optical nutation, free induction, and photon echo, in the acetylene-filled PCFs.

II. EXPERIMENTAL SETUP

In the presented experiments we utilized a pumped-through acetylene-filled hollow-core PCF cell. For a detailed description of the experimental configuration see our earlier publication [6]; here we only mention that in our all-fiber gas cell a piece of the hollow-core PCF was optically coupled to conventional single-mode SMF28 fibers inside standard ceramic ferrules. Both ferrules had transverse cuts that ensured connection to a gas evacuation system and to a cylinder with acetylene. The cell was fabricated from a 2.6-m-long piece of a HC-1550-04 single-mode hollow-core PCF (of NKT Photonics, Inc.) with a 10.6(±0.3)-μm core diameter and a mode field diameter of 7.5 μm at the central transmission wavelength 1550 nm. The typical optical transmission of the PCF-SMF28 connections was ≈0.3–0.5. The vacuum system utilized in the reported experiments was fabricated completely from stainless steel and the pressure in it was measured using a capacitance barometer from MKS Instruments, Inc.

The optical part of the all-fiber setup is shown in Fig. 1. The optical pulse source consisted of a temperature-controlled cw distributed feedback (DFB) semiconductor laser with a central operation wavelength of 1530.3 nm, a high-contrast electro-optic amplitude modulator from Photline, and a 980-nm pumped 11-m-long erbium-doped fiber (EDF)

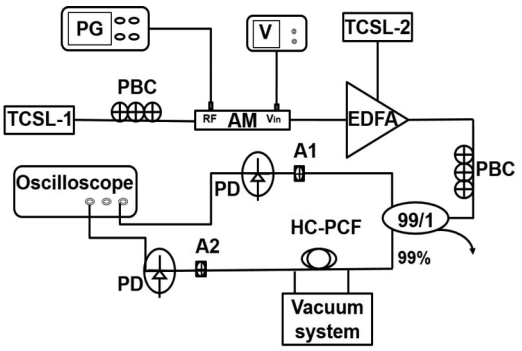

FIG. 1. Optical part of the all-fiber experimental setup (TCSL: semiconductor laser; AM: amplitude electro-optic modulator; PBC: polarization controller; A1 and A2: attenuators; PD: photodiode; V: voltage source; PG: pulse generator; EDFA: erbium doped fiber amplifier).

optical amplifier. This experimental configuration ensured nanosecond pulses with up to 5 W peak light power at the input end of the acetylene-filled PCF. Fast (7 GHz) photodiodes were used for real-time monitoring of the shapes and amplitudes of incident and transmitted light pulses. The majority of the below-presented data were obtained for the $P9$ acetylene absorption line centered at $\lambda = 1530.37$ nm [8]; however, similar effects were also observed for other absorption lines, in particular, for $P7$, $P8$, and $P10$. No significant difference was observed between the experimental data obtained with conventional commercial and purified (99.5% purity) acetylene.

Direct measurements of the absorption spectra under the acetylene pressures lower than 0.35 Torr resulted in a nearly Gaussian spectral profile of this line with the full width at half maximum (FWHM) of about 500 MHz [2,6]. For comparison, the FWHM spectral width of the utilized semiconductor cw DFB laser was measured to be below 3 MHz.

III. EXPERIMENTAL RESULTS

To reach the maximum possible relaxation times necessary for observation of coherent optical light-molecule interactions, one has to reduce the acetylene pressure to minimize the influence of intermolecule collisions. In order to evaluate this contribution, we have measured the dependence of the acetylene cell (incoherent) saturation power P_{sat} on the gas pressure [6]. This characteristic value is typically defined [12] as a stationary incident light power P for which the optical absorption coefficient α of the experimental fiber cell becomes one half of its initial, not-saturated value α_0:

$$\alpha(P) = \frac{\alpha_0}{1 + P/P_{\text{sat}}}. \tag{1}$$

Note that the cell optical density $\alpha_0 L$, which is proportional to the gas pressure p (measured in the vacuum system chamber), characterizes the acetylene density in the cell. Direct measurements have shown that for low pressures ($\leq$0.05 Torr) P_{sat} was about 0.18 mW. It constantly grew with increase of the acetylene density and reached approximately double value at the cell optical density $\alpha_0 L \approx 1$, which approximately corresponds to a pressure of 0.2 Torr. In approximation of

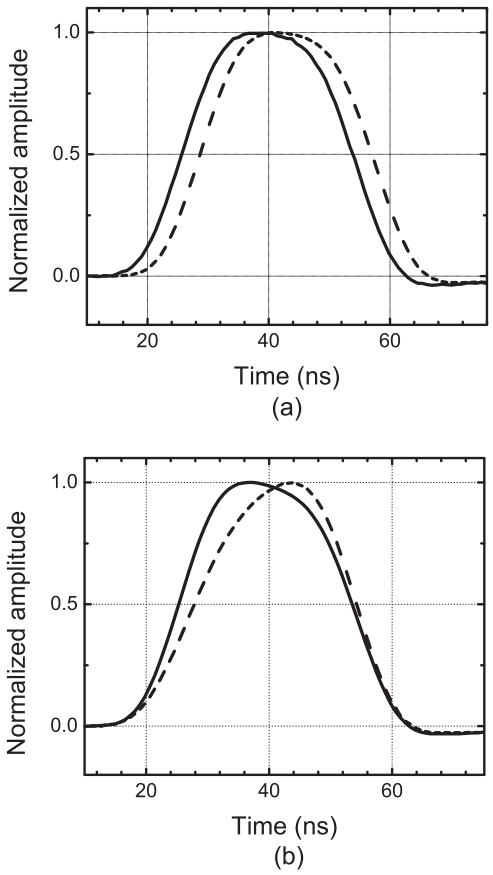

FIG. 2. Normalized oscilloscope traces of Gaussian-like 30-ns input (solid lines) and output (dashed lines) pulse shapes when laser wavelength is tuned (a) outside and (b) inside the acetylene absorption line ($P_{\text{in,max}} = 1.6$ W, $\alpha_0 L = 2.8$). In (b) time delay between the detection channels for the input and output signals is compensated.

strong collisions (when $T_1 \approx T_2$) this means reduction of T_2 by a factor of $\sqrt{2}$.

Note that because the mode field diameter ($\approx$7.5 μm) is $\approx$25% smaller than the hollow-core diameter, the maximum T_2 determined by the time of a coherent interaction of acetylene molecules with the excitation light beam can even be shorter than the time between the collisions with the core walls. Taking all these factors into account, and also that not all molecules cross the fiber axes traveling from one wall to another, gives us the following estimation for $T_2 \approx 10$ ns at the above-mentioned typical cell optical density.

Oscilloscope traces of the normalized input and output optical pulses at the wavelength tuned outside of the acetylene $P9$ absorption line are shown in Fig. 2(a). Similar output pulse shapes were also observed for the acetylene absorption wavelength in the cell with very low gas pressure. The shift between these two reference profiles was used in the processing of the experimental data to eliminate temporal shifts between the input and output pulse profiles caused by different optical path lengths in the detection channels.

As reported in [6], a considerable delay of the weight center of the transmitted pulse is observed if incident pulses of an intermediate duration ($\approx$30 ns) having a smooth Gaussian-like profile are used; see Fig. 2(b). This effect is ensured by

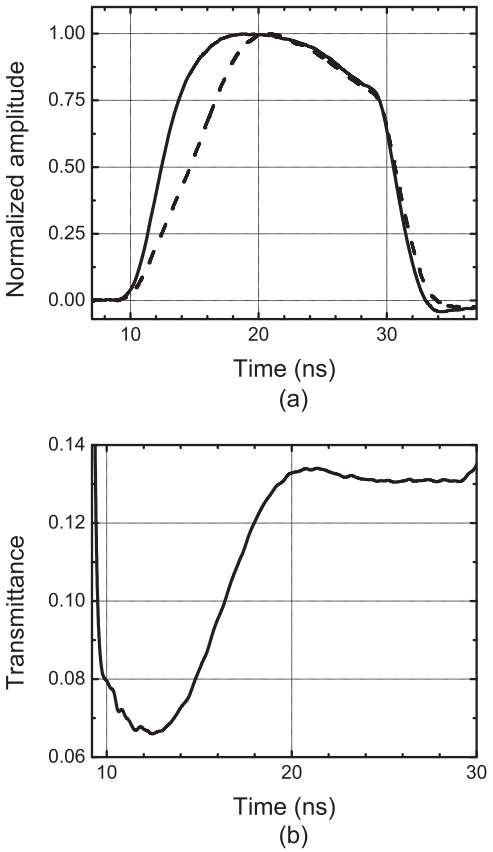

FIG. 3. (a) Normalized oscilloscope traces of 20-ns input (solid line) and output (dashed line) pulses with steep fronts, with the laser wavelength tuned inside the acetylene absorption line and with compensated time delay ($P_{\text{in,max}} = 3$ W, $\alpha_0 L = 0.9$). Curve (b) presents temporal dependence of the gas cell transmittance T.

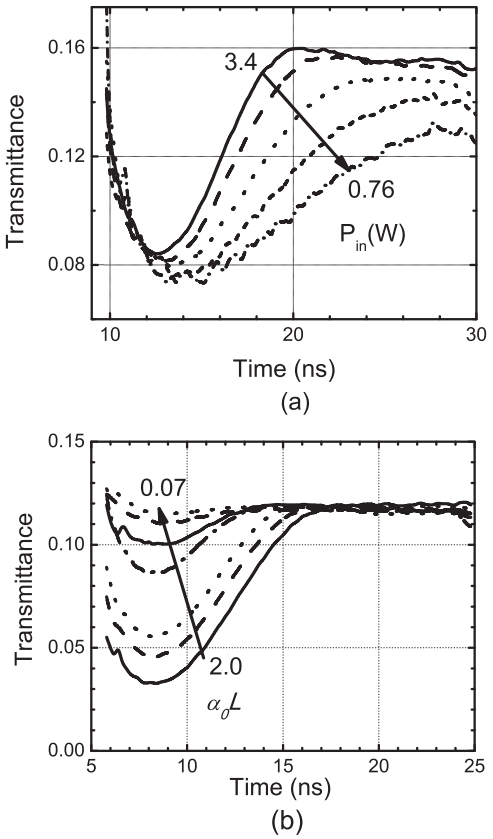

FIG. 4. (a) Time dependences of the cell optical transmittance for 20-ns pulses at fixed optical density $\alpha_0 L = 0.9$ and different maximum input powers P_{in} (W): 0.76, 1.14, 1.72, 2.63, and 3.4. (b) Similar dependences obtained at fixed input power $P_{\text{in}} \approx 3.2$ W for different cell optical densities (0.07, 0.15, 0.3, 0.55, 0.9, 1.3, and 2.0).

effective absorption of the light power from the leading front of the incident pulse. On the opposite, the trailing pulse front is less absorbed by the saturated (by this moment) material, which leads to deformation of the pulse shape and an effective delay of its weight center. This effect of the "slow light propagation" is well explained [13] by the conventional model of the incoherent light interaction with a saturable two-level system [12].

The minimum front rise or decay time determined by the utilized Tektronix AFG3252C pulse generator was about 2 ns (or 1 ns when the generator is controlled via PC). The normalized oscilloscope traces of the rectangularlike 20-ns-long input (with short 2 ns fronts) and output pulses in the case when the laser wavelength is tuned to the acetylene absorption line are presented in Fig. 3(a).

The experimentally observed acetylene cell behavior in the case when an input pulse with such sharp leading front is used proves to be essentially different. To compensate for the not-ideally rectangular shape of the incident light pulse, we calculated the ratio between the output and input pulse intensities, i.e., the cell optical transmittance T shown in Fig. 3(b). One can clearly see that there is an oscillation; i.e., at first transmittance goes down from a relatively high initial level and only after this it starts to grow.

A set of similar transmittance profiles observed for the cell with a fixed optical density at different input pulse powers is presented in Fig. 4(a). Similar profiles obtained for a fixed light power but for different acetylene pressures (i.e., initial cell optical densities) are shown in Fig. 4(b). It is evident that the oscillation period grows with decreasing input pulse power, and the oscillation depth grows with the acetylene pressure.

We attribute these oscillations to the optical nutation effect typical for propagation of light through a coherent two-level optical medium [11]. In bulk gas media (in particular, in SF_6 at a wavelength of 10.6 μm and in $C^{13}H_2F$ and NH_2D at 0.97 μm; see [14] and [15], respectively) this effect was observed in the late 1960s to early 1970s. Note that this type of oscillating behavior differs significantly from the resonant light propagation through an incoherently saturated two-level medium when the transmittance of the material grows continuously with time.

The quite large modulation depth in the experimentally observed optical nutation effect also gives us hope that we can also observe other coherent effects, and in particular free induction and photon echo [11]. Unlike the optical nutation, in these two effects the same radiation of the excited acetylene molecules is observed in absence of the coherent transmitted excitation pulses and, for this reason, these effects are significantly weaker.

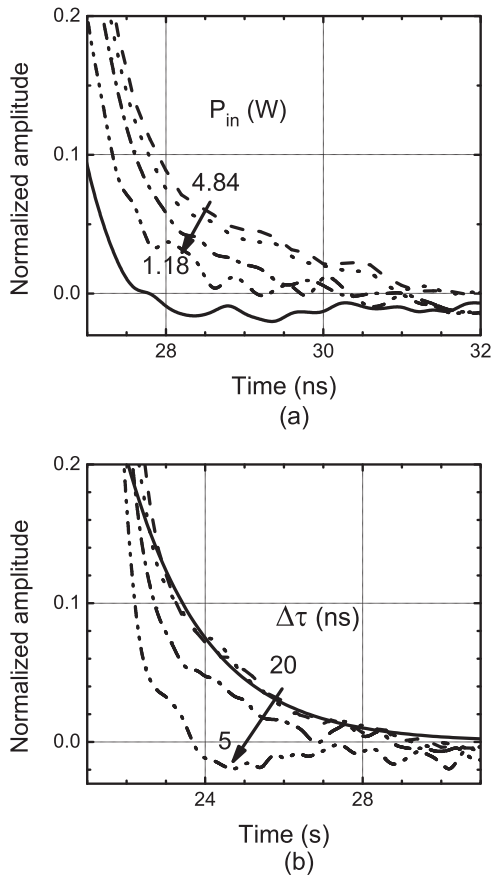

FIG. 5. (a) Normalized free induction signal profiles observed for 10-ns excitation pulses with maximum input power (W): 1.2, 2.6, 3.9, and 4.8 (the solid line shows the normalized trailing edge of the input pulse). (b) The same for input power 4.84 W of the excitation pulses with duration (ns): 5, 10, 15, and 20 (the solid line shows exponential decay with characteristic time 2 ns).

The optical free induction [11] demonstrates itself as a "tail" of the coherent radiation from the medium after the incident light pulse is shut off. A set of oscilloscope traces of such signals observed for the acetylene cell with a fixed optical density ($\alpha_0 L \sim 1.7$) is presented in Fig. 5(a). For comparison, this figure also shows a much shorter trailing front of the input light pulse (the solid line). Such short trailing fronts are also observed in the transmitted pulses when the wavelength is tuned out of the acetylene absorption line. Figure 5(b) shows free induction signals excited by input pulses of a constant peak power ($\approx$5 W) but of different duration.

The most impressive-looking nonstationary coherent optical effect observed under the monochromatic excitation is, probably, the photon echo [11]. It is observed as a light pulse coherently radiated by the medium which was preilluminated by a sequence of two closely spaced coherent light pulses. Figure 6(a) shows the output photon echo signals which we experimentally observed from our acetylene-filled PCF cell with optical density $\alpha_0 L \approx 1.8$ excited with a pair of collinearly propagating 2-ns pulses. The inset to this figure presents amplified echo signals observed for different input pulse delays $\Delta\tau_{12} = 4.4$, 5.0, 5.9, and 6.6 ns. For comparison, Fig. 6(b) shows similar responses from the same cell when the wavelength is tuned outside of the acetylene absorption line. Figures 6(c) and 6(d) show dependences of the detected echo amplitude versus $\Delta\tau_{12}$ and maximum pulse power, respectively.

IV. DISCUSSION

In the following discussion of the experimental results the value of relaxation time T_2 is of major importance. For this reason, we start with the evaluation of this parameter from our data on two-pulse photon echo. It is well known that the intensity of this echo signal decays as $\approx \exp(-4\Delta\tau_{12}/T_2)$ [11,16]. This allows us to evaluate T_2 from Fig. 6(c) as $\approx$8 ns, which proves to be in reasonable agreement with the above-presented theoretical evaluation ($\approx$10 ns) for similar conditions of the experiment.

As to the nutation signal (Figs. 3 and 4), the observed coherent oscillations occur approximately at the Rabi frequency $\Omega_R = E\mu/\hbar$, which is proportional to the product of the light electric field E and the dipole moment μ of the optical transition under consideration [11]. These oscillations are associated with periodic change of the amplitude and the sign in the radiating electric dipole moment of the coherently excited molecules. As a result, a decrease in the transmitted light (that corresponds to the destructive interference of the incident light and that irradiated by the molecules) is followed by its increase (constructive interference) and so on. At the very first moment of the illumination, the coherent transmission is to be equal to 1 (no absorption at all), since the dipole moment of the system at the base energy level is zero.

Reduction of the incident light power results in a corresponding reduction in the frequency of the oscillations observed in the transmitted signal. And indeed, a similar trend is observed in the experimental data shown in Fig. 4(a). On the other hand, the increment in the cell optical density yields an increase in the oscillation depth of the transmitted signal [see Fig. 4(b)], as would be expected, since the optical nutation signal grows proportionally to the number of the acetylene molecules interacting with the incident light wave.

In the case of a narrow absorption line and when there is no relaxation, the optical nutation oscillations would continue without any relaxation [see the dashed line in Fig. 7(a), which presents the temporal behavior of the sample transmittance]. In reality, these oscillations in transmittance decay with the characteristic time of transverse relaxation T_2 because of the loss of memory of the oscillators (or quantum transitions) about their initial phases [11]. Decaying oscillations expected for different products $\Omega_R T_2$ are shown in Fig. 7(a).

From the experimental curve corresponding to the maximum incident light power used ($\approx$3.4 W) in Fig. 4(a) one can approximately estimate the maximum Rabi oscillations frequency as $\approx$100 MHz, that for $T_2 \approx 8$ ns results in $\Omega_R T_2 \approx 5$. Comparison of the experimentally observed oscillations [Fig. 4(a)] and the theoretical dependences [Fig. 7(a)] obviously shows significant discrepancy.

Another reason for the nutation oscillations' attenuation is associated with significant inhomogeneous broadening of the absorption line and with nonuniformity of the gas volume illumination [16]. The limit case of the inhomogeneously

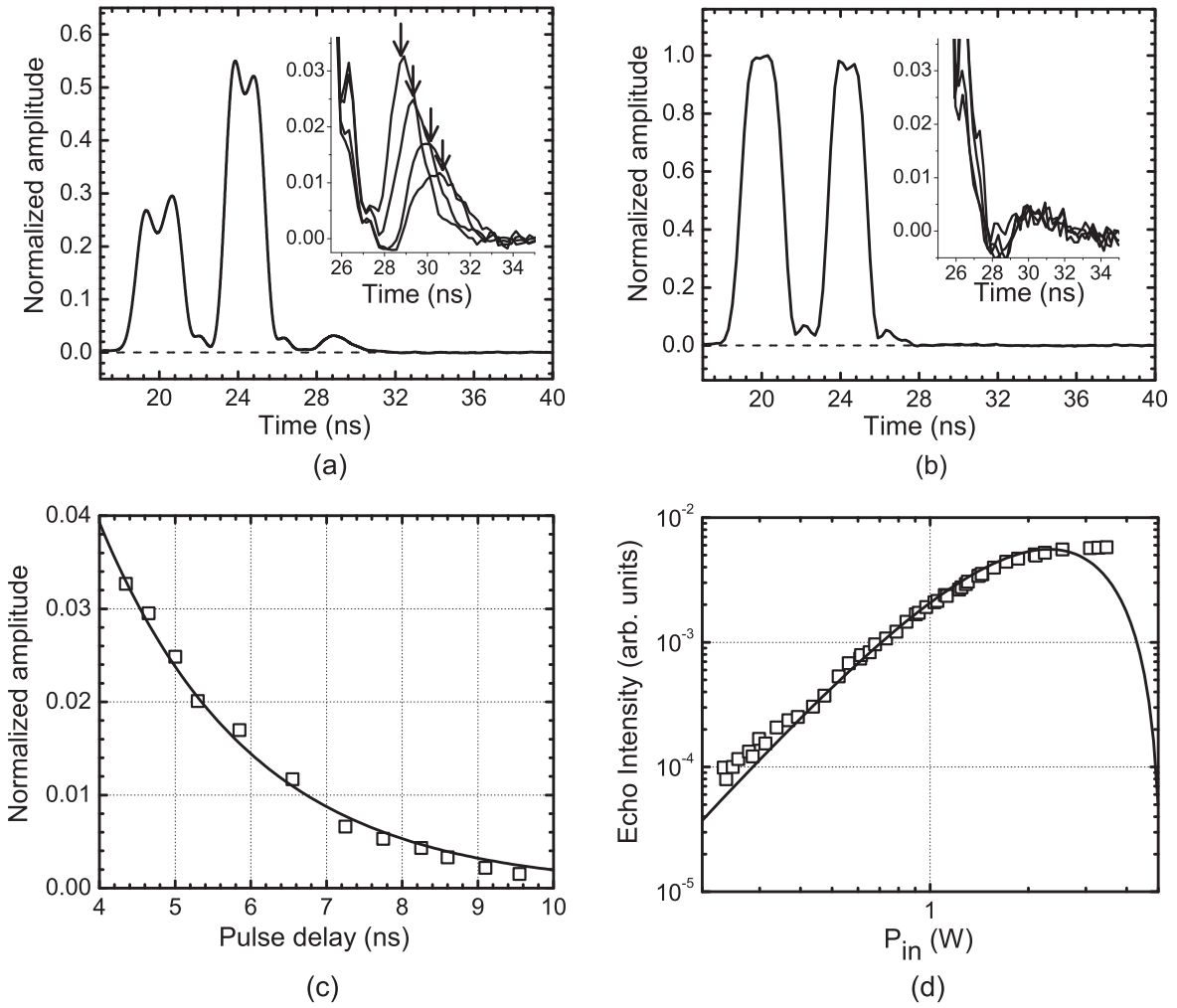

FIG. 6. (a) Echo signal observed for two-pulse excitation (inset shows amplified echo signals for different input pulse separations of 4.4, 5.0, 5.9, and 6.6 ns, arrows show expected echo positions). (b) Similar response observed at the wavelength tuned outside of the absorption line. Echo amplitude (c) as a function of the excitation pulse separation (solid line presents exponential decay with characteristic time 2 ns), and (d) as a function of the excitation pulse power (solid line presents theoretical dependence).

broadened absorption linewidth significantly larger than the Rabi frequency was considered, in particular, in [16]. In our case the Rabi frequency (≈100 MHz) is rather close to the linewidth (≈500 MHz) and our numerical simulation shows that approximation of a narrow absorption line is still rather adequate.

We believe that, like nonuniformity of illumination [16], the random orientation of acetylene molecules in the gas cell results in a significant attenuation of the nutation oscillations. Indeed, every molecule experiences dipole interaction with the collinear component of the linearly polarized electric field in the light wave only [17] and has its own Rabi frequency in the range from its maximum value Ω_R to 0. Direct averaging over the molecule orientations results in the following expression for the time-dependent profile of the optical nutation signal:

$$1 - C\frac{\sin(\Omega_R t) - \Omega_R t\cos(\Omega_R t)}{(\Omega_R t)^2}, \qquad (2)$$

which substitutes the conventional factor $[1 - C\sin(\Omega_R t)]$ expected for a set of collinearly oriented molecules. In these expressions coefficient C characterizing the optical nutation modulation depth depends on the oscillator strength, concentration of active molecules, and cell length.

Figure 7(b) demonstrates additional attenuation of nutation oscillations due to a random orientation of molecules alone for a simple model case of $C = 0.5$. Note that this coefficient cannot be associated with some particular optical density of the sample directly. Indeed, the optical absorption also includes in an essential way the transverse relaxation time T_2, which does not influence in a direct way the modulation depth of the nutation oscillations, at least, at their beginning.

One can see that the random orientation of the gas molecules reduces by a factor of ≈2.5 the maximum modulation depth of the oscillations. The comparison of those experimentally observed (Figs. 3 and 4) with the theoretically predicted for $\Omega_R T_2 = 5$ results, obviously, in a much better agreement. Nonuniform distributions of the light intensity along the fiber length and across the fiber mode also contribute to this effect [16].

Note also that Fig. 4(a) also shows clear growth of the stationary saturation level of the cell transmittance with the incident light power. Since this incoherent process is governed

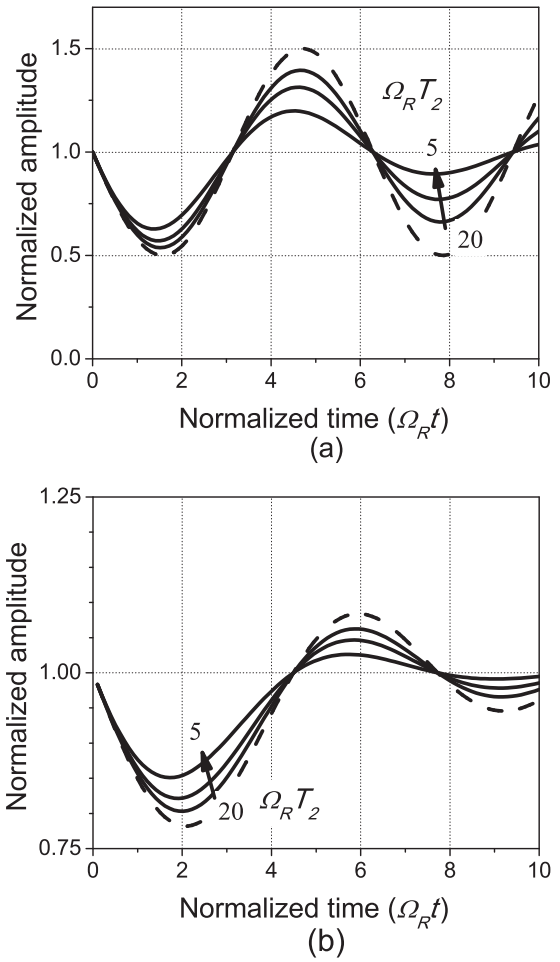

FIG. 7. Theoretical shapes of the normalized optical nutation signal (a) for collinearly oriented dipoles, and (b) for randomly oriented dipoles. Dashed lines present case without relaxation, solid lines correspond to $\Omega_R T_2 = 20$, 10, and 5 (with corresponding reduction of the oscillation depth).

by the longitudinal relaxation time, the presented experimental curves confirm proximity of T_1 to T_2 in our case.

As to the free induction signal, its amplitude is proportional to the area A of the exciting pulse (i.e., the product of the Rabi frequency and the pulse duration $\Delta\tau$ [11]), at least, in the approximation of small areas $A \leq 1$ rad. As a result, the oscillation amplitude of the free induction signal observed at fixed $\Delta\tau$ is proportional to the pulse maximal power, which was observed in the experiments with 10 ns excitation pulses; see Fig. 5(a).

In the above-presented experiments of observation of free induction, the relatively long excitation pulses with the spectral width narrower than that of the absorption line (500 MHz) were used. In this case the number of the effectively excited molecules has to decrease with increasing pulse duration $\Delta\tau$. However, the pulse area A grows linearly with $\Delta\tau$, and, as a result, the experimentally observed maximum free induction power is not affected by the pulse duration.

The parameter influenced by $\Delta\tau$ in this case is the free induction signal duration: The longer the excitation pulse, the narrower its spectral width, and the longer the free induction response. As a result, it can usually be expected that for small pulse area $A \leq 1$ rad the free induction signal duration after the exciting pulse is shut off is close to $\Delta\tau/2$. Except for the shortest excitation pulse duration $\Delta\tau = 5$ ns, the free induction response observed in our experiments was, however, much shorter than the exciting pulse and was practically independent of its duration; see Fig. 5(b).

This effect can be explained by the following argument proposed in [18]. When the excitation pulse duration is longer than the transverse relaxation time, the spectral linewidth of the effectively excited molecules is determined mainly by T_2, which leads to the additional (to the conventional transverse relaxation with time T_2 relaxation of the free induction amplitude proportional to $\exp(-t/T_2)$. And indeed, the exponential relaxation with the characteristic time 2 ns ($\approx T_2/4$) was experimentally observed for all free induction signal intensities excited with pulses of duration ≥ 10 ns; see Fig. 5(b). Note also that the no-monotonic response presented in this figure for short 5-ns excitation pulse shows behavior reported in [19] earlier.

As to the experimentally observed photon echo signal, it demonstrated the expected exponential decay with the time delay between the excitation pulses, which was utilized above for evaluation of T_2. The intensity of the experimentally observed echo signal demonstrated the expected superquadratic (with approximate power index ≈ 2.3) dependence on the pulse power. For comparison in Fig. 6(d) we also show the expected theoretical dependence of the echo intensity versus excitation pulse power obtained in the approximation of undepleted pulse power. The experimentally observed saturation of the echo amplitude as well as clear nutation oscillations in the transmitted excitation pulses confirms that the areas of the excitation pulses reached the optimum value close to $2\pi/3$ in these experiments.

When approximated to the center of the first excitation pulse, the echo intensity normalized to the incident pulse intensity equals 0.3. This means that the maximal free induction amplitude after the first excitation pulse has the normalized amplitude about ≈ 0.5. In the nutation response such coherent irradiation of the molecules has to reduce the normalized intensity of the transmitted pulse to the value $\approx (1-0.5)^2 = 0.25$, which was, indeed, observed experimentally in the transmitted pulse presented in Fig. 6(a).

V. CONCLUSION

Summarizing, experimental observations of nonstationary coherent interactions, namely, the optical nutation, free induction, and the photon echo, for the two-level optical transition of the acetylene in the hollow-core PCF at room temperature are reported. The presented experiments were performed in the all-fiber optical configuration at the acetylene $P9$ transition wavelength 1530.37 nm. For the maximal incident optical power of 3.4 W the Rabi frequency was found to be about ≈ 100 MHz. The transverse relaxation time ≈ 8 ns governed by the intermolecule collisions and by their limited stay inside the effective modal area was observed under typical acetylene pressures < 0.4 Torr. To explain the experimentally observed rapid attenuation of the nutation oscillations, we have applied the model of randomly oriented classical acetylene molecules.

Obvious advantages of the experimental configuration we use for observation of the above-mentioned coherent optical effects are (i) a possibility of an all-fiber and completely closed implementation (which also reduces necessary peak light powers), (ii) matching with the wavelength region of modern fiber optical communication systems, and (iii) operation at room temperature. All these factors can, in particular, be attractive for applications of the photon echo effect to quantum computing widely discussed at present [20].

ACKNOWLEDGMENT

The work of P.A. was partially supported by the President Council of the Russian Federation, Grant No. SP-1900-2012.5

[1] F. Benabid, F. Couny, J. C. Knight, T. A. Birks, and P. St J. Russell, Nature **434**, 488 (2005).
[2] S. Ghosh, J. E. Sharping, D. G. Ouzounov, and A. L. Gaeta, Phys. Rev. Lett. **94**, 093902 (2005).
[3] J. Henningsen, J. Hald, and J. C. Petersen, Opt. Express **13**, 10475 (2005).
[4] F. Couny, P. S. Light, F. Benabid, and P. St. J. Russell, Opt. Commun. **263**, 28 (2006).
[5] N. V. Wheeler, P. S. Light, F. Couny, and F. Benabid, J. Lightwave Technol. **28**, 870 (2010).
[6] P. Agruzov, A. Shamray, M. Ocegueda Miramontes, E. Hernández Hernández, and S. Stepanov, Appl. Phys. B **108**, 827 (2012).
[7] M. de Labachelerie, K. Nakagawa, and M. Ohtsu, Opt. Lett. **19**, 840 (1994).
[8] W. C. Swann and S. L. Gilbert, J. Opt. Soc. Am. B **17**, 1263 (2000).
[9] P. Th. Marty, J. Morel, and Th. Feurer, Opt. Lett. **36**, 3569 (2011).
[10] P. Th. Marty, J. Morel, and Th. Feurer, Opt. Express **18**, 26821 (2010).
[11] L. Allen and J. H. Eberly, *Optical Resonance and Two-Level Atoms* (Dover Publications, New York, 1975).
[12] A. E. Siegman, *Lasers* (University Science Books, Sausalito, CA, 1986).
[13] A. C. Selden, Br. J. Appl. Phys. **18**, 743 (1967).
[14] G. B. Hocker and C. L. Tang, Phys. Rev. Lett. **21**, 591 (1968).
[15] R. G. Brewer and R. L. Shoemaker, Phys. Rev. Lett. **27**, 631 (1971).
[16] R. L. Shoemaker, in *Laser and Coherence Spectroscopy*, edited by J. I. Steinfeld (Plenum Press, New York, 1978), pp. 197–371.
[17] P. P. Feofilov, *The Physical Basis of Polarized Emission: Polarized Luminescence of Atoms, Molecules, and Crystals* (Consultants Bureau, New York, 1961).
[18] R. G. Brewer and R. L. Shoemaker, Phys. Rev. A **6**, 2001 (1972).
[19] A. Z. Genack, R. M. Macfarlane, and R. G. Brewer, Phys. Rev. Lett. **37**, 1078 (1976).
[20] W. Tittel, M. Afzelius, T. Chaneliere, R. L. Cone, S. Kroll, S. A. Moiseev, and M. Sellars, Laser Photonics Rev. **4**, 244 (2010).